# Potent and Selective α-Ketoheterocycle-Based Inhibitors of the Anandamide and Oleamide Catabolizing Enzyme, Fatty Acid Amide Hydrolase

F. Anthony Romero,[†,‡] Wu Du,[†,‡] Inkyu Hwang,[†,‡] Thomas J. Rayl,[†,‡] F. Scott Kimball,[†,‡] Donmienne Leung,[§,‡] Heather S. Hoover,[§,‡] Richard L. Apodaca,[⊥] J. Guy Breitenbucher,[⊥] Benjamin F. Cravatt,[§,‡] and Dale L. Boger*,[†,‡]

*Departments of Chemistry, Cell Biology, and The Skaggs Institute for Chemical Biology, The Scripps Research Institute, 10550 North Torrey Pines Road, La Jolla, California 92037, and Johnson & Johnson Pharmaceutical Research and Development, L.L.C., 3210 Merryfield Row, San Diego, California 92121*

A study of the structure−activity relationships (SAR) of **2f** (OL-135), a potent inhibitor of fatty acid amide hydrolase (FAAH), is detailed, targeting the 5-position of the oxazole. Examination of a series of substituted benzene derivatives (**12**−**14**) revealed that the optimal position for substitution was the meta-position with selected members approaching or exceeding the potency of **2f**. Concurrent with these studies, the effect of substitution on the pyridine ring of **2f** was also examined. A series of small, nonaromatic C5-substituents was also explored and revealed that the $K_i$ follows a well-defined correlation with the Hammett $\sigma_p$ constant ($\rho = 3.01$, $R^2 = 0.91$) in which electron-withdrawing substituents enhance potency, leading to inhibitors with $K_i$s as low as 400 pM (**20n**). Proteomic-wide screening of the inhibitors revealed that most are exquisitely selective for FAAH over all other mammalian proteases, reversing the 100-fold preference of **20a** (C5 substituent = H) for the enzyme TGH.

Fatty acid amides are an important new class of lipid signaling molecules that modulate a number of physiological processes. Two endogenous fatty acid amides, anandamide (**1a**)[1] and oleamide (**1b**),[2−4] have emerged as prototypical members of this class that serve as chemical messengers (Figure 1). Anandamide (**1a**), which was only discovered a little more than a decade ago and is the most recognizable member of the endogenous fatty acid ethanolamides,[5] binds and activates both the central type-1 (CB1) and peripheral type-2 (CB2) cannabinoid receptors. Anandamide (**1a**), and members of the cannabinoid family,[6] have been implicated in the modulation of nociception,[7−9] feeding,[10,11] emesis, anxiety,[12] cell proliferation,[13,14] inflammation,[15] memory,[16] and neuroprotection after brain injury.[17] Thus, the cannabinoids have clinical relevance for analgesia, anxiety, epilepsy, cachexia, cancer, and Alzheimer's disease as well as other neurodegenerative diseases.[18−20]

Oleamide (**1b**) was found to accumulate in the cerebrospinal fluid of animals under conditions of sleep deprivation and to induce physiological sleep in a dose dependent manner where it reduced motility, shortened the sleep induction period, and lengthened the time spent in slow wave sleep 2 at the expense of wakening.[2,4] In a structurally specific manner, it was found to modulate serotonergic systems[21−23] and GABAergic transmission,[24,25] block glial gap junction cell−cell communication,[26,27] decrease body temperature and locomotor activity,[28] and exhibit the characteristic in vivo analgesic and cannabinoid behavorial effects of anandamide,[21,29] albeit without direct cannabinoid receptor activation. It has been suggested that the cannabinoid behavorial effects of oleamide (**1b**) may be mediated through an as yet unknown distinct pharmacological target.[24] Because oleamide (**1b**) may play a critical role in sleep, it may provide an exciting therapeutic potential for the develop-
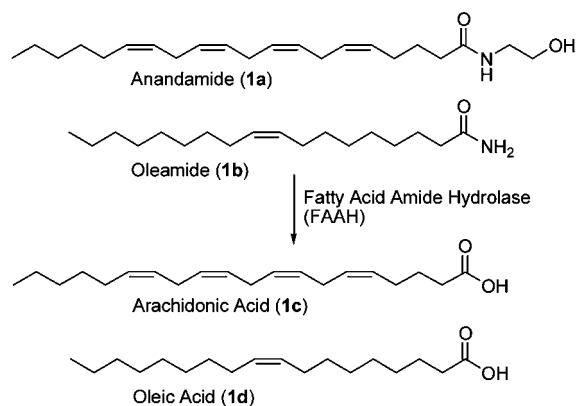


**Figure 1.** Substrates of fatty acid amide hydrolase (FAAH).

ment of sleep aids that induce physiological sleep lacking the side effects of the sedative-hypnotics (e.g., benzodiazepene class), which include rebound insomnia, anterograde amnesia, and suicide abuse potential.

The pharmacological action of anandamide (**1a**) and oleamide (**1b**) is terminated by the enzyme fatty acid amide hydrolase (FAAH,[a] Figure 1).[30−33] Fatty acid amide hydrolase is an integral membrane protein that degrades the fatty acid amide family of endogenous signaling lipids.[34,35] Its central nervous system distribution indicates that it degrades neuromodulating fatty acid amides at their sites of action and is intimately involved in their regulation.[36] Fatty acid amide hydrolase is currently the only characterized mammalian enzyme that is in the amidase signature family bearing an unusual catalytic Ser-Ser-Lys triad.[30,33,37−39] Recently, the crystal structure of FAAH cocrystallized with an irreversibly bound arachidonyl fluorophosphonate confirmed its unusual catalytic triad and provided structural details of this enzyme.[30] Studies with FAAH knockout mice have not only shown that this enzyme is a key regulator of fatty acid amide signaling in vivo but that there are also

* Corresponding author. Phone: 858-784-7522. Fax: 858-784-7550. E-mail: boger@scripps.edu.
† Department of Chemistry, The Scripps Research Institute.
‡ Department of Cell Biology, The Scripps Research Institute.
§ The Skaggs Institute for Chemical Biology, The Scripps Research Institute.
⊥ Johnson & Johnson Pharmaceutical Research and Development, L.L.C.

[a] Abbreviations: FAAH, fatty acid amide hydrolase; TGH, triacylglycerol hydrolase.
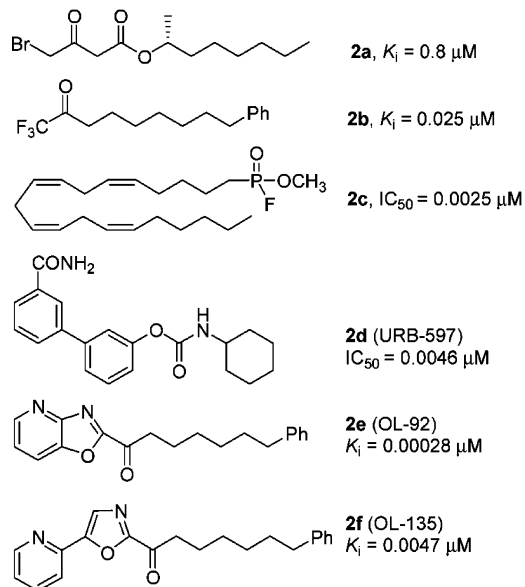
**Figure 2.** Examples of FAAH inhibitors.

**Scheme 1**



significant augmented behavioral responses (e.g., increased analgesia, hypomotility, catalepsy) to administered anandamide (**1a**) and oleamide (**1b**) resulting from increased brain levels of the fatty acid amides that correlated with a CB1-dependent analgesic phenotype.[40−43] As such, FAAH has emerged as an interesting new therapeutic target for a range of clinical disorders.[6,44]

Due to the potential therapeutic relevance of inhibiting FAAH, there has been increasing interest in developing potent and selective inhibitors of this enzyme (Figure 2).[12,45−60] These include the discovery that the endogenous sleep-inducing molecule 2-octyl α-bromoacetoacetate (**2a**) is an effective FAAH inhibitor,[55] a series of reversible inhibitors bearing an electrophilic ketone[46,54,56,61] (e.g., trifluoromethyl ketone **2b**) that have not proven selective for FAAH over other mammalian serine hydrolases[62] and a set of irreversible inhibitors[48−50,52,53] (e.g., fluorophosphonate **2c** and sulfonyl fluorides). Recently, two classes of compounds have been disclosed that provide significant advances in the development of an inhibitor with therapeutic potential. One class is the aryl carbamates (e.g., **2d**) that acylate an active site catalytic serine and which were shown to exhibit anxiolytic activity and induce analgesia.[12,57−59,63,64] However, the selectivity of such aryl carbamate inhibitors is low, and recent studies show that either no or minimal selectivity is achieved (e.g., other targets of **2d** are carboxylesterase 6 and triacylglyceride hydrolase).[64−66] A second class is the α-keto-heterocycle-based inhibitors of which some are extraordinarily potent (e.g., **2e** and **2f**).[45,47,51,62,67] These competitive inhibitors bind to FAAH via reversible hemiketal formation with an active site serine and are not only potent and extraordinarily selective for FAAH versus other mammalian serine hydrolases,[45,62] but many are efficacious in vivo and promote analgesia.[66,68]

From these latter studies, **2f** has emerged as an advanced lead.[45,51,62,66−68] It has been shown that **2f** is a potent FAAH inhibitor ($K_i$ = 4.7 nM) that induces analgesia by raising endogenous anandamide levels,[66] is more than 300-fold selective for FAAH over any other serine hydrolase,[45] lacks significant offsite target activity when surveyed against a full panel of receptors and enzymes (Cerep assay profiling), and does not significantly inhibit the common P450 metabolism enzymes (3A4, 2C9, 2D6) or the human ether-a-go-go related gene (hERG). As part of a continuing program in developing FAAH inhibitors, it was of interest to more fully explore the structure−
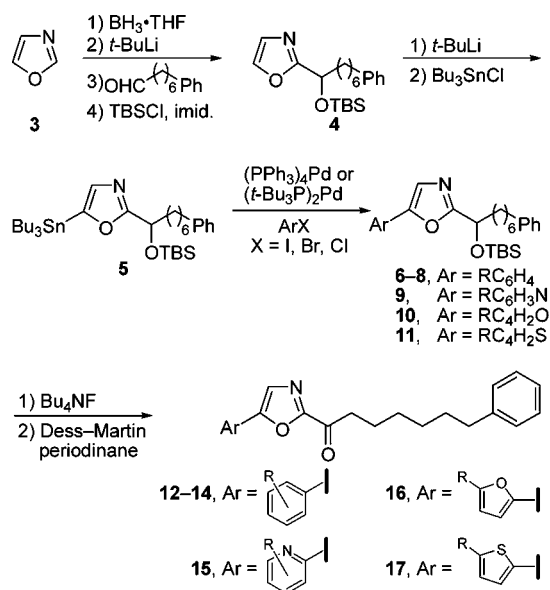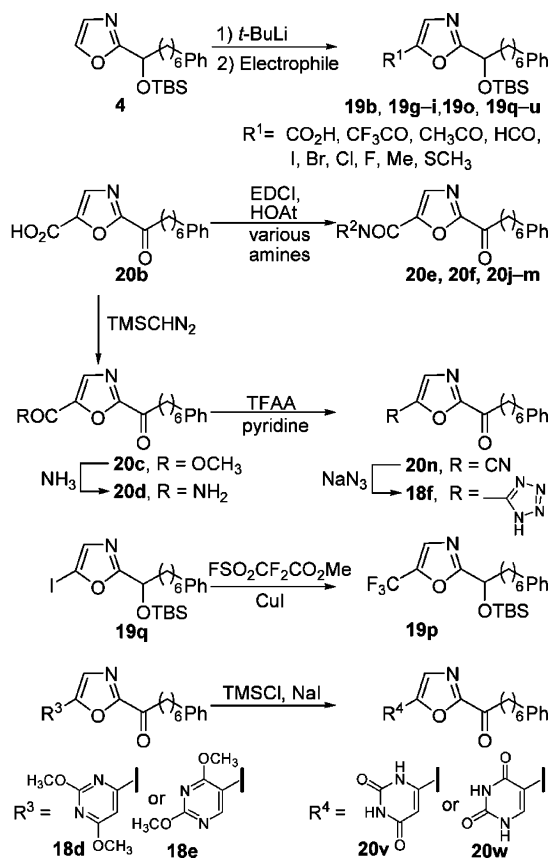
activity relationships (SAR) of **2f** targeting the 5-position of the central oxazole ring (e.g., various aryl and nonaromatic substituents). Herein we report the synthesis and evaluation of this more extensive series of 5-substituted 7-phenyl-1-(oxazol-2-yl)heptan-1-ones along with the results of proteome-wide selectivity screening of candidate inhibitors.[69]

**Chemistry.** Key to the divergent synthesis of the inhibitors was the preparation of the intermediate **4**[45] from which all the requisite compounds could be synthesized. Intermediate **4** was obtained by Vedejs oxazole metalation,[70] condensation with 7-phenylheptanal, and TBS protection of the resulting alcohol. Selective C5-oxazole lithiation[71] of **4** followed by treatment with Bu$_3$SnCl afforded stannane **5**. Stille coupling[72] of stannane **5** with a systematic series of aryl halides produced **6−11**, which could be readily converted to the corresponding 5-aryl substi-tuted 7-phenyl-1-(oxazol-2-yl)heptan-1-ones **12−17** via TBS deprotection and oxidation of the liberated alcohol with Dess−Martin periodinane (Scheme 1).[73]

The synthesis of the candidate inhibitors that bear a nonaro-matic C5-oxazole substituent is summarized in Scheme 2. After selective C5-oxazole lithiation, **4** was treated with a range of electrophiles (CO$_2$(g), CF$_3$CON(CH$_3$)$_2$, CH$_3$CON(CH$_3$)$_2$, DMF, I$_2$, Br$_2$, N-chlorosuccinimide, N-fluorobenzenesulfonimide, CH$_3$I, dimethyl disulfide) to give **19b**, **19g−i**, **19o**, and **19q−u**, many of which served as precursors to additional candidate inhibitors bearing further modified C5-substituents. Carboxylic acid **20b** was directly converted to a series of amides (**20e**, **20f**, **20j−m**; RNH$_2$ or R$_2$NH, EDCI, and HOAt) as well as to its correspond-ing methyl ester **20c** by treatment with TMSCHN$_2$. The ester **20c** was converted to the carboxamide **20d** by treatment with methanolic ammonia. Carboxamide **20d** was dehydrated with TFAA and pyridine to provide nitrile **20n**, which in turn was converted to the tetrazole **18f** upon treatment with NaN$_3$. Using a method developed by Chen et al., iodide **19q** was transformed to **19p** (FSO$_2$CF$_2$CO$_2$CH$_3$, CuI) bearing a C5 trifluoromethyl substituent.[74,75] The O-methyl pyrimidine derivatives (**18d**, **18e**) were treated with TMSCl and NaI to yield the uracil analogues (**20v**, **20w**). In each case, deprotection of the TBS ether followed by Dess−Martin periodinane oxidation of the liberated alcohol yielded the corresponding α-ketoheterocycles.

**Enzyme Assay.** Enzyme assays were performed at 20−23 °C with purified recombinant rat FAAH expressed in *E. coli*[76]
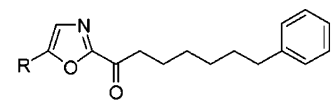
**Scheme 2**





Figure 3. α-Keto oxazole inhibitors of FAAH.

| compd | R | $K_i$, µM |
|---|---|---|
| 2f | 2-pyridyl | 0.0047 |
| 2g | 2-furyl | 0.012 |
| 2h | 2-thienyl | 0.055 |
| 2i | phenyl | 0.08 |



**2i** R = H, $K_i$ = 0.08 µM

|  | $K_i$ (µM) | | |
|---|---|---|---|
| R | 2-position | 3-position | 4-position |
| NO$_2$ | 0.13 (12a) | 0.028 (13a) | 0.05 (14a) |
| NH$_2$ | 0.75 (12b) | 0.019 (13b) | 0.09 (14b) |
| CO$_2$CH$_3$ | 0.06 (12c) | 0.012 (13c) | 0.04 (14c) |
| CO$_2$H | 6.0 (12d) | 0.005 (13d) | 0.06 (14d) |
| F | 0.11 (12e) | 0.05 (13e) | 0.062 (14e) |
| OCH$_3$ | 0.4 (12f) | 0.04 (13f) | 0.1 (14f) |
| OH | 0.17 (12g) | 0.05 (13g) | 0.14 (14g) |
| SO$_2$NH$_2$ | 1.5 (12h) | 0.002 (13h) | 0.01 (14h) |
| CONH$_2$ | 0.3 (12i) | 0.006 (13i) | 0.01 (14i) |
| COCF$_3$ | 5.0 (12j) | 0.016 (13j) | 0.065 (14j) |
| CN | 0.13 (12k) | 0.015 (13k) | 0.04 (14k) |

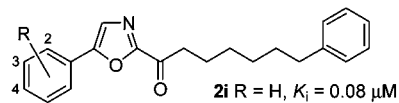Figure 4. Effect of substitution on the benzene ring.

(unless indicated otherwise) or with solubilized COS-7 membrane extracts from cells transiently transfected with human FAAH cDNA[32] (where specifically indicated) in a buffer of 125 mM Tris/1 mM EDTA/0.2% glycerol/0.02% Triton X-100/0.4 mM HEPES, pH 9.0 buffer.[55] The initial rates of hydrolysis ($\leq 10-20\%$ reaction) were monitored using enzyme concentrations (typically 2 nM) at least two times below the measured $K_i$ by following the breakdown of ^{14}C-oleamide and $K_i$s (standard deviations provided in Supporting Information Tables) established as described (Dixon plot).[47] Lineweaver–Burk analysis previously established reversible, competitive inhibition for **2f** and related compounds.[45]

**Results and Discussion**

**Aryl Substitution.** We previously disclosed a small set of 5-aryl-substituted 7-phenyl-1-(oxazol-2-yl)heptan-1-ones,[45] and this study defined a smooth increase in inhibitory potency as the hydrogen-bonding capability of the 5-aryl substituent increased (**2h** to **2g** to **2f**, Figure 3). Complete removal of the pyridine nitrogen of **2f**, providing compound **2i**, resulted in a significant loss of FAAH inhibitory potency ($K_i$ = 80 nM, 140 nM reported in ref 45). This loss of inhibitory potency proved consistent with a loss in binding affinity due to a hydrogen-bond interaction. Monte Carlo simulations of **2f** suggested that the pyridine nitrogen of **2f** is involved in a direct hydrogen-bond to the hydroxyl of Thr236 and the protonated nitrogen of Lys142.[45,77] As depicted in the modeling studies and as evidenced by the tolerated variance in the positioning of such pyridyl hydrogen-bond acceptors in a series of FAAH inhibitors,[45] the interaction is between the conformationally mobile catalytic residues at the active site of the enzyme and is adaptable to the positioning of the hydrogen-bond as well as the residue (Ser217 and Lys142) involved. To further explore

such interactions, a systematic series of benzene derivatives bearing substituents on the 2-, 3-, and 4-positions was examined (Figure 4). Several important trends emerged from the examination of this series. Substitution at the 2-position (**12** series) reduced inhibitory potency relative to the unsubstituted phenyl derivative **2i** (R = H, $K_i$ = 80 nM), whereas substitution at the 3- (**13** series) or 4-positions (**14** series) moderately (up to 8-fold for 4-substitution) or significantly (up to 40-fold for 3-substitution) enhanced the inhibitory potency. Without exception, the rank order FAAH inhibitory potency for each substituent is 3-substitution > 4-substitution > 2-substitution. It is likely that the 2-substituents disfavor the near coplanar arrangement of the phenyl and oxazole rings observed in modeling studies,[45,77] leading to the lower inhibitory potencies for this series versus **2i** (R = H) itself. The exceptions to this generalization are small (**12e**, R = F; **12k**, R = CN) electron-withdrawing (**12c**, R = CO$_2$CH$_3$) substituents that approach or match the activity of **2i**.

The 3- and 4-positions exhibit similar substituent trends, but with the 3-substituent providing inhibitors as much as 10-fold more potent than the corresponding 4-substituent (typically 2 to 3-fold). Although the generalizations are not fully defined with this set of substituents, the increases in inhibitory potency relative to **2i** were greatest with electron-withdrawing versus electron-donating substituents (e.g., OH, OCH$_3$, NH$_2$) and appear to benefit further if the electron-withdrawing substituent embodies both hydrogen-bond acceptor and donor capabilities. It is possible that the electronic character of the substituent may be responsible for or contribute to the changes in $K_i$ values especially for the 4-substituents. Here, the electron-donating substituents (NH$_2$, OCH$_3$, OH) provided inhibitors less active than the parent phenyl derivative **2i**, whereas electron-withdrawing substituents enhanced the activity. However, the fact that the substituent effects do not smoothly follow rank order trends and that the most potent series constitute the meta (not para or ortho) substituents suggests that the electronic effect of the substituent is not the only source of the modulated binding
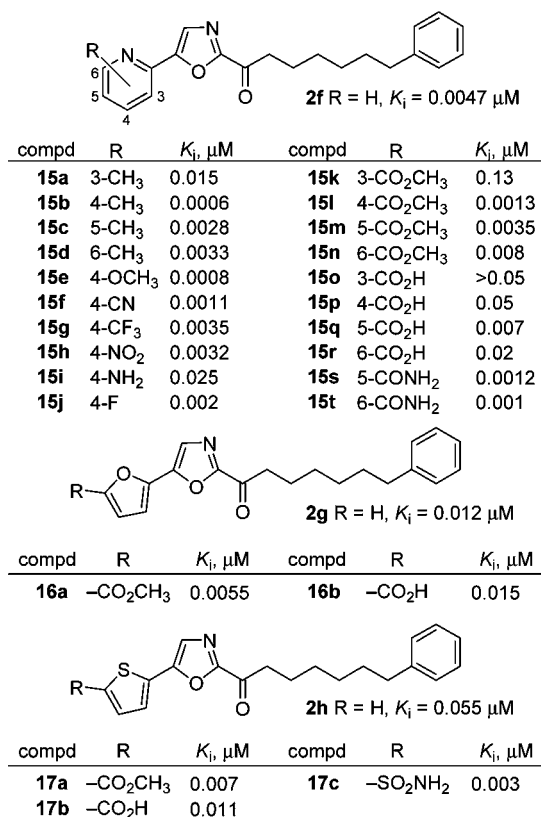
**2f** R = H, $K_i$ = 0.0047 μM

| compd | R | $K_i$, μM | compd | R | $K_i$, μM |
|-------|------|---------|-------|----------|---------|
| **15a** | 3-CH₃ | 0.015 | **15k** | 3-CO₂CH₃ | 0.13 |
| **15b** | 4-CH₃ | 0.0006 | **15l** | 4-CO₂CH₃ | 0.0013 |
| **15c** | 5-CH₃ | 0.0028 | **15m** | 5-CO₂CH₃ | 0.0035 |
| **15d** | 6-CH₃ | 0.0033 | **15n** | 6-CO₂CH₃ | 0.008 |
| **15e** | 4-OCH₃ | 0.0008 | **15o** | 3-CO₂H | >0.05 |
| **15f** | 4-CN | 0.0011 | **15p** | 4-CO₂H | 0.05 |
| **15g** | 4-CF₃ | 0.0035 | **15q** | 5-CO₂H | 0.007 |
| **15h** | 4-NO₂ | 0.0032 | **15r** | 6-CO₂H | 0.02 |
| **15i** | 4-NH₂ | 0.025 | **15s** | 5-CONH₂ | 0.0012 |
| **15j** | 4-F | 0.002 | **15t** | 6-CONH₂ | 0.001 |

**2g** R = H, $K_i$ = 0.012 μM

| compd | R | $K_i$, μM | compd | R | $K_i$, μM |
|-------|----------|---------|-------|--------|---------|
| **16a** | –CO₂CH₃ | 0.0055 | **16b** | –CO₂H | 0.015 |

**2h** R = H, $K_i$ = 0.055 μM

| compd | R | $K_i$, μM | compd | R | $K_i$, μM |
|-------|----------|---------|-------|----------|---------|
| **17a** | –CO₂CH₃ | 0.007 | **17c** | –SO₂NH₂ | 0.003 |
| **17b** | –CO₂H | 0.011 | | | |

**Figure 5.** Effect of substitution on a pyridine, furan, and thiophene ring.

affinities. Notably, several of the 3-substituted derivatives (**13** series) approach or match the potency of **2f** ($K_i$ = 4.7 nM), which benefits from the presence of the pyridyl group hydrogen-bond acceptor (20-fold increase over phenyl derivative **2i**), without the deliberate use of a weakly basic heterocyclic nitrogen as a hydrogen-bond acceptor.[45] The carboxylic acid of **13d**, carboxamide of **13i**, and primary sulfonamide of **13h** appear to be in an optimal position in the active site to benefit from stabilizing binding interactions that match the effect of the pyridine nitrogen of **2f**. Notably, **13d** and **13i** have FAAH inhibitory potencies indistinguishable from **2f**, whereas **13h** is twice as potent as **2f**.

Concurrent with these studies, the effect of substitution on the pyridine ring of **2f** was examined (Figure 5). Initially, a methyl scan of the pyridine subunit was performed with placement of a methyl group at each available site (3-, 4-, 5-, and 6-positions). Whereas methyl substitution at the 3-position (**15a**) led to a modest 3-fold decrease in inhibitory potency, substitution at the 4-, 5-, and 6- positions (**15b**–**d**) led to inhibitors that were 1.5 to 8-fold more potent than the parent **2f**. With the optimal substitution being at the 4-position (**15b**), several additional substituents (**15e**–**j**) were examined at this position and all led to modest increased inhibitory potency (up to 6-fold) compared to **2f** (except **15i**, 4-NH₂). None of the derivatives in this 4-substituted series (**15a**–**j**) quite matched the potency of **15b** (4-CH₃), and interestingly this increased potency relative to **2f** proved relatively independent of whether this 4-substituent was an electron-donating or electron-withdrawing group that might significantly alter the pyridyl nitrogen basicity and hydrogen-bond capability. Nonetheless and excluding **15i**, the substituent effects do roughly mirror a trend that might reflect their impact on the hydrogen-bond acceptor capability of the pyridine nitrogen (CH₃, OCH₃ > CO₂CH₃, CN,

CF₃, NO₂), albeit within a narrow range and not with a rank order that strictly reflects the electronic properties of the pyridyl substituent.

Since the study with the substituted benzene derivatives (Figure 4) revealed that it was possible to place substituents in the meta-position of the benzene ring (**13d**, **13h**, **13i**) and obtain inhibitors that were more potent or equipotent to **2f**, we explored the addition of these substituents (e.g., CO₂CH₃, CO₂H, CONH₂; **15k**–**t**) to the pyridine ring of **2f** to establish whether this would lead to a further enhancement in inhibitory potency. As expected, substitution at the pyridyl 3-position (ortho-substitution) with either a methyl ester (**15k**) or carboxylic acid (**15o**) resulted in decreased inhibitory potency analogous to observations in the **12** series (Figure 4). Methyl ester substitution at the remaining positions provided inhibitors that were more potent than the corresponding phenyl series (**13c**, **14c**) with the 4- and 5-substitution matching or exceeding the potency of **2f** by 3- and 1.3-fold, respectively, and 6-substitution approaching, but not enhancing, that of **2f**. Notably, this places the C4 methyl ester (**15l**) among the most potent of the 4-substituents and among the most potent inhibitors of the series. Importantly, this incorporation of the pyridine nitrogen into **13c** and **14c** enhances inhibitory potency 10-fold, which is consistent with its proposed role as a hydrogen-bond acceptor approaching the 20-fold enhancement observed with **2f** versus phenyl derivative **2i**. Similarly, addition of a carboxamide to the pyridyl 5- (**15s**) or 6-position (**15t**) resulted in significant increases in inhibition (2.5- and 4-fold, respectively relative to **2f**), providing the most potent inhibitors in the series and compounds that are more than 5-fold more potent than the corresponding phenyl series (**13i**, **14i**). Finally, the substitution of a carboxylic acid at the 4-, 5-, and 6-positions of **2f** provided effective inhibitors of FAAH with **15q** (5-CO₂H) and **15r** (6-CO₂H) approaching the potency of **2f**. This is especially significant since the in vitro assays for FAAH inhibition are conducted at pH 9 where the inhibitors are fully ionized, likely masking their true inhibitory potency at physiological pH. Thus, not only were many of the candidate inhibitors as potent or more potent than **2f**, but several of these compounds (**15q**–**t**) contain moieties that would be expected to productively alter the physicochemical properties of **2f** (e.g., water solubility). With these observations, we examined the incorporation of these substituents on both the furan and thiophene rings of **2g** and **2h** (**16a**,**b**, **17a**–**c**). All led to similar or increased inhibitory potency as compared to parent inhibitors **2g** or **2h** of which **17c** is notably 18 times more potent than parent **2h**.

Additional aryl substituents that were examined in this study are summarized in Figure 6 and complement those disclosed (e.g., **18a**–**c**) along with **2f**.[45] The addition of methoxy groups to the pyrimidine ring of **18a** and **18c** (**18d**, **18e**) had no effect on inhibitory potency relative to **18a** and **18c**. Tetrazole **18f** experienced a 12-fold decrease in inhibitory potency compared to **2f**, although it is still more potent than phenyl derivative **2i**. A significant decrease in inhibitory potency was observed for dimer **18g**.

**Small, Nonaromatic Substituents.** The results of the studies with the aryl substituents (vide supra), as well as previous studies,[45] indicated that typically electron-deficient aryl groups bearing substituents capable of hydrogen-bonding at the 5-position of the oxazole of these α-ketoheterocycles are important for imparting low nanomolar inhibitory potency. As such, we were interested in establishing if this would be observed with nonaromatic substituents that were also capable of hydrogen-bonding. Consequently, a representative series of such candidate

**Figure 6.** Effect of additional aryl groups. Compounds **18a**−**c** are from a previous study.[45] See Supporting Information for a more extensive table which includes previous 5-heterocyclic substituents.



**Figure 7.** Effect of nonaromatic substituents.

inhibitors bearing electron-withdrawing substituents was prepared and examined for FAAH inhibition (Figure 7). Although the carboxylic acid **20b** led to only a small increase in inhibitory potency relative to **20a** (R = H), all other carboxylic acid and ketone derivatives (**20c**−**i**, **20n**) exhibited excellent inhibiton substantially exceeding the potency of **20a** and approaching or exceeding the activity of **2f** with **20n** ($K_i$ = 400 pM) emerging as a picomolar inhibitor. Notably, even though a 5-fold loss of potency is observed with the carboxylic acid **20b** as compared to **2f** in an assay artificially conducted at pH 9, **20b** is still a very potent inhibitor of FAAH that qualitatively possesses different physicochemical properties (e.g., solubility) than **2f**. A small, but systematic exploration of the amide derivatives (**20j**−**m**) illustrated a smooth increase in inhibitory potency as the polarity of the six-membered ring decreased. Analogous to prior observations,[45] substitution on the oxazole with a 5-methyl substitutent (**20o**) resulted in a significant loss in activity relative
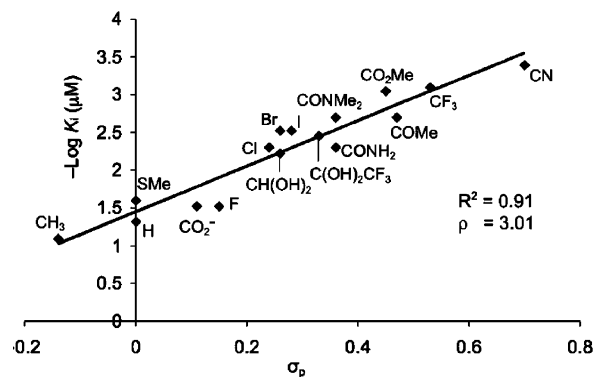


**Figure 8.** −Log $K_i$ ($\mu$M) versus $\sigma_p$.

to **20a** (R = H). In contrast and unexpectedly, derivatives **20p**−**t** which contain C5-substituents that are not regarded as hydrogen-bond acceptors all exhibited potencies greater than that of **20a** (R = H) and approaching or exceeding that of **2f**. Especially noteworthy was the observation that **20p** (R = CF$_3$) exhibited extraordinarily potent inhibition of FAAH ($K_i$ = 800 pM). Moreover, this series exhibited a well-defined trend for the halide substituents (CF$_3$ > I ≥ Br > Cl > F) that tracks with their electron-withdrawing properties. With this in mind, a correlation plot of the inhibition (−log $K_i$) versus the Hammett $\sigma_p$ constant for this entire series was constructed (Figure 8).[61] The activity of this series, which constitutes a set of relatively small substituents that can occupy accessible space in the FAAH active site, was found to follow a well-defined correlation with $\sigma_p$ ($R^2$ = 0.91) in which the electron-withdrawing substituents predictably enhance the inhibitory potency. In addition, this substituent effect was established to be large ($\rho$ = 3.01), resulting in a 1000-fold increase in $K_i$ per unit change in $\sigma_p$, which indicates that the electronic character of the substituent is the dominant factor contributing to the differences in binding affinity. Presumably, this arises from the increased electrophilic character of the C2 carbonyl imparted by the electron-withdrawing C5 substituent that leads to an increased strength of the covalent bond formed with the Ser241 OH, enhancing the stability of the adduct and slowing the off-rate, thus lowering the $K_i$ value. The definition of this fundamental relationship between the $K_i$ and substituent property ($\sigma_p$) permits the prediction of an expected $K_i$ value. With confidence, we can assert that the carboxylic acid (**20b**) binds FAAH as the carboxylate anion (CO$_2^-$ vs CO$_2$H, $\sigma_p$ = 0.11 vs 0.44) under the conditions of the assay (from the $K_i$ value, pH 9). Even more interestingly, we are able to establish that both the aldehyde **20i** and trifluoromethyl ketone **20h** exist in solution as gem diols (at C5, but not C2; ^{1}H and ^{13}C NMR, Supporting Information) and inhibit the enzyme with potencies ($K_i$ = 6 and 3.5 nM) at a level more consistent with this C5 substituent gem diol versus carbonyl active site binding and providing the first $\sigma_p$ estimates for such substituents (0.26 for CH(OH)$_2$ and 0.33 for C(OH)$_2$CF$_3$). On occasion, an anomalous $\sigma_p$ of 0.22 is reported or used for CHO (vs 0.42) that may more accurately reflect an analogous but unrecognized gem diol. That is, the correlation between $\sigma_p$ and $K_i$ is sufficiently dependable that deviations from expectations can be utilized to establish features of active site binding that are not a priori known. Similarly, with the correlation in hand, several of the potent inhibitors in Figure 7 were retrospectively prepared and examined based solely on this relationship. Notably, **20c**, **20n**, and **20p** bearing the strongest electron-withdrawing substituents display subnanomolar inhibitory potency. Aside from its role in establishing the potent FAAH inhibitors detailed herein, to our knowledge
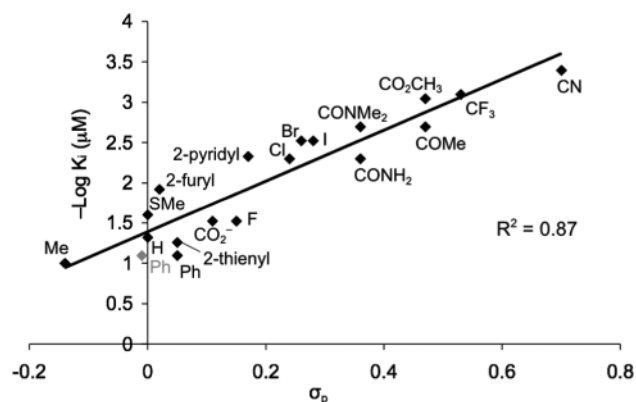
**Figure 9.**  $-\text{Log } K_i$ ($\mu$M) versus $\sigma_p$.



| compd | R | $K_i$, $\mu$M | compd | R | $K_i$, $\mu$M |
|---|---|---|---|---|---|
| **21a** | $-CN$ | 4.2 | **21f** | | 2.5 |
| **21b** | $-CF_3$ | 2.3 | | | |
| **21c** | $-CO_2CH_3$ | 2.0 | | | |
| **21d** | $-CONH_2$ | 25 | | | |
| **21e** | $-CON(CH_3)_2$ | 16 | | | |



| compd | R | $K_i$, $\mu$M | compd | R | $K_i$, $\mu$M |
|---|---|---|---|---|---|
| **21g** | 6-$CO_2CH_3$ | 2.3 | **21j** | 5-$CO_2H$ | 45 |
| **21h** | 5-$CO_2CH_3$ | >10 | **21k** | 6-$CONH_2$ | 2.1 |
| **21i** | 6-$CO_2H$ | >10 | **21l** | 5-$CONH_2$ | 3.0 |

**Figure 10.**  The effect of removing the electrophilic carbonyl.

this also represents the first delineation of a fundamental substituent effect for such $\alpha$-ketoheterocycles that has eluded experimental verification[78,79] in studies conducted to date.[80]

While additional substituent features can and will further modulate the binding affinity of the candidate inhibitors (e.g., H-bonding, hydrophobic, or steric interactions), the magnitude of the electronic effect of the substituent ($\rho = 3.01$) on the activity of a conjugated $\alpha$-ketoheterocycle ($K_i$) suggests the latter will dominate, especially with small substituents. For example, if one tries to incorporate the **20j**$-$**m** carboxamide series into the correlation, each is significantly less potent than predicted indicating that the larger six-membered ring amides embody steric (**20j**$-$**m**) and additional hydrophilic (**20j** and **20k**) characteristics that incrementally destabilize inhibitor binding. More interestingly, placing the larger phenyl ($K_i = 80$ nM, $\sigma_p = 0.05$ or $-0.01$), 2-furyl ($K_i = 12$ nM, $\sigma_p = 0.02$), 2-thienyl ($K_i = 55$ nM, $\sigma_p = 0.05$), and 2-pyridyl ($K_i = 4.7$ nM, $\sigma_p = 0.17$) substituents (disclosed in ref 45) on the correlation plot (Figure 9) revealed several interesting features. The 2-pyridyl and 2-thienyl substituents appear to fit the correlation well, but this may in fact be misleading. The phenyl substituent, which is larger than the substituents depicted in Figure 8, exhibits a $K_i$ notably weaker than the correlation would predict. However, even here and with the choice of $\sigma_p = -0.01$ (vs 0.05), it provides a correlation that is not unreasonable. Although there may be several explanations for this behavior, we have interpreted this to indicate that there may be destabilizing (presumably steric) interactions that accompany binding of such a large C5 substituent in the active site. In contrast, the 2-thienyl (slightly weaker than predicted) and 2-pyridyl (slightly more potent than predicted) substituents exhibit $K_i$s that appear to be predicted by the correlation but are anomalous when compared to the phenyl or furyl substituent. We attribute this to a key stabilizing active site hydrogen bond (discussed earlier in modeling studies, ref 45) which compensates for the destabilizing steric interactions progressively enhancing the potency of the inhibitors bearing the 2-thienyl and 2-pyridyl substituents such that 2-thienyl approaches and 2-pyridyl exceeds the correlation prediction. Consistent with this, the 2-furyl substituent also positively deviates from the correlation consistent with its relative H-bonding capabilities. Interestingly, the H-bonded pyridyl nitrogen (partial protonation) would make this substituent a stronger electron-withdrawing substituent. Whether the productive deviation of the 2-pyridyl substituent is best interpreted simply as benefiting from an additional stabilizing H-bond, or whether this represents an enhanced electronic effect of the H-bonded substituent, is not a question that can be answered with this study. However, it does suggest that the modeled[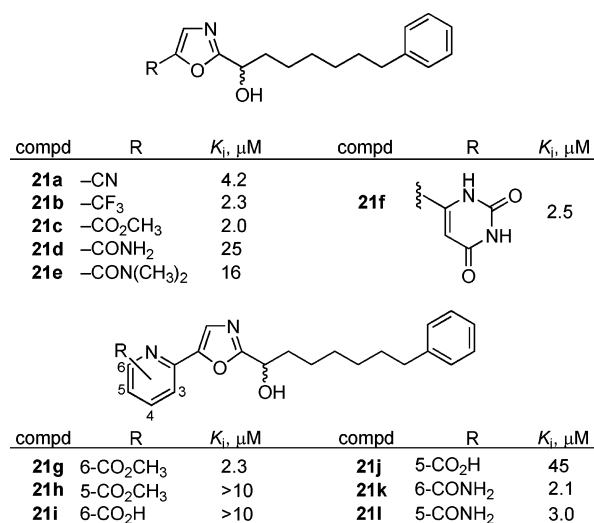45] H-bonded array is responsible for its improved potency and productive deviation from the correlation. Importantly, its deviation from the correlation does not negate the correlation, and the correlation does not negate the prior modeling observations with the 2-pyridyl substituent. Rather, its productive deviation from the correlation highlights a special character of this substituent and allows the identification of active site binding features that are not a priori known. Similarly, the substituted phenyl (**12**$-$**14**) and pyridyl series (**15**) cluster in regions surrounding the parent phenyl or pyridyl substituent. The latter series exhibits less variation in the $K_i$, whereas the former exhibits a greater variation and the trends reflect the expected impact of an added electron-withdrawing substituent, albeit within a range where it is further modulated by additional features that affect binding site affinity.

Finally, two uracil derivatives (**20v**, **20w**) were also examined in this series, and only **20v** exhibited excellent inhibitory potency.

**The Electrophilic Carbonyl.** Consistent with past observations,[45] the alcohol precursors to several of the $\alpha$-ketoheterocycles (**21a**$-$**l**) were examined and found to be approximately $10^4$$-$$10^3$ times less potent than the corresponding ketone (Figure 10). However, it should be noted that in many instances DMSO stock solutions of compounds **21a**$-$**21l** were reevaluated by analytical LCMS after biological testing and were found to contain small (0.1%) amounts of a material that was consistent in mass and retention time to the corresponding ketone and that increased in relative amount upon sample storage. In other cases, the ketone peak was not seen (detection limits of ca. 0.02%). Given the very high potency of the ketones ($10^3$ to $10^4$-fold more potent than the alcohols) and the tendency of the alcohols to slowly autooxidize to the corresponding ketones (data not shown), it is beyond current technical and analytical detection limits to conclusively rule out the possibility that the activity of these alcohol samples is due to trace amounts of ketone impurities.

**Inhibition of Recombinant Human FAAH.** Rat and human FAAH are very homologous (84% sequence identity), exhibit near identical substrate selectivities and inhibitor sensitivities in studies disclosed to date,[47] and embody an identical amidase signature sequence, suggesting the observations made with rat FAAH would be analogous to those made with the human enzyme. Consequently, key inhibitors in the series were examined against the human enzyme, and consistent with previous observations[45] were found to exhibit the same relative and absolute potencies (Figure 11).

| compd | $K_i$, μM (human) | $K_i$, μM (rat) |
|-------|-------------------|-----------------|
| **15q** | 0.008 | 0.007 |
| **15r** | 0.026 | 0.02 |
| **20b** | 0.032 | 0.03 |
| **20n** | 0.001 | 0.0004 |

**Figure 11.** Inhibition of recombinant human fatty acid amide hydrolase.

| compd | $K_i$, μM | FAAH | KIAA1363 | TGH |
|-------|-----------|------|----------|-----|
| **2f** | 0.0047 | 0.002 | >100 (>50000) | 0.6 (300) |
| **13d** | 0.005 | 1.4 | >100 (>70) | >100 (>70) |
| **13h** | 0.002 | 0.4 | >100 (>200) | 0.2 (0.5) |
| **13i** | 0.006 | 2.7 | >100 (>40) | >100 (40) |
| **15b** | 0.0006 | 0.001 | >100 (>100000) | 2 (2000) |
| **15e** | 0.0008 | 0.0017 | >100 (>59000) | 0.5 (300) |
| **15f** | 0.0011 | 0.0008 | >100 (>125000) | 0.4 (500) |
| **15g** | 0.0035 | 0.0015 | >100 (>67000) | 2 (1300) |
| **15h** | 0.0032 | 0.0016 | >100 (>63000) | 0.2 (125) |
| **15i** | 0.025 | 0.34 | >100 (>300) | 34 (100) |
| **15j** | 0.002 | 0.0025 | >100 (>40000) | 0.6 (240) |
| **15l** | 0.0013 | 0.0006 | >100 (>170000) | 0.9 (2000) |
| **15q** | 0.007 | 0.05 | >100 (>2000) | 3 (60) |
| **15r** | 0.02 | 0.1 | >100 (>1000) | >100 (>1000) |
| **16b** | 0.015 | 0.85 | >100 (>120) | >100 (>120) |
| **18d** | 0.005 | 0.4 | >100 (>250) | 0.07 (0.2) |
| **18e** | 0.026 | 9 | >100 (>11) | 3 (0.3) |
| **20a** | 0.048 | 2.5 | 19 (8) | 0.02 (0.008) |
| **20b** | 0.030 | 0.97 | >100 (>100) | >100 (>100) |
| **20c** | 0.0009 | 0.03 | >100 (>3300) | 0.3 (10) |
| **20d** | 0.0045 | 0.35 | >100 (>300) | 7 (20) |
| **20m** | 0.008 | 0.45 | >100 (>200) | 8 (20) |
| **20n** | 0.0004 | 0.0065 | >100 (>15400) | 0.02 (3) |
| **20p** | 0.0008 | 0.077 | >100 (>1300) | 0.2 (3) |
| **20r** | 0.008 | 0.19 | 13 (70) | 0.1 (0.5) |
| **20v** | 0.012 | 0.005 | >100 (>20000) | 30 (6200) |
| **20w** | 0.35 | 0.68 | >100 (>150) | 30 (40) |

**Figure 12.** Selectivity screening; IC$_{50}$, μM (selectivity).

**Selectivity Screening.** Early assessments of α-ketoheterocycle inhibitors of FAAH against possible competitive enzymes (e.g., phospholipase A2, ceramidase) revealed no inhibition. Consequently, a method for proteomic-wide screening capable of globally profiling all mammalian serine hydrolases was developed,[69] and studies have shown that the α-ketoheterocycle class of inhibitors are exquisitely selective for FAAH.[45,62,66] However, two enzymes did emerge as potential competitive targets: triacylglycerol hydrolase (TGH) and an uncharacterized membrane-associated hydrolase that lacks known substrates or function (KIAA1363). In this screen, IC$_{50}$ values are typically higher than the measured $K_i$ values, but the relative potency, the magnitude of binding affinity differences, and the rank order binding determined in the assay parallels that established by standard substrate assays.

Summarized in Figure 12 are the results of the selectivity screening of selected candidate inhibitors. In general, these new α-ketoheterocycle inhibitors were very selective for FAAH over TGH and KIAA1361 except **13h**, **18d**, **18e**, **20a**, and **20r**, which were selective for TGH. Thus, substitution at the C5 oxazole position with either aromatic or nonaromatic substituents provides selective inhibitors compared to unsubstituted **20a** which itself is 100-fold selective for TGH over FAAH. Consistent with prior observations, incorporation of a substituted 2-pyridyl group at C5 provided superb selectivities (**15** series, >100-fold selective) analogous to that observed with **2f** itself, whereas the incorporation of substituted phenyl groups (**13** series) or nonaryl substituents (**20** series) at C5 provided more modest FAAH selectivities. Most notably, substitution of a carboxylic acid either directly on the oxazole ring (**20b**) or on the 5-aryl moiety (**13d**, **15q**, **15r**, **16b**) appears to impart even greater selectivity for FAAH providing inhibitors (>50−1000-

fold selectivity) that fail to inhibit either TGH or KIAA1363. Notably, this reversal of selectivity from **20a** (>10⁴ change in relative activity) occurs with both increases in affinity for FAAH and disruption of affinity for TGH and KIAA1363, both of which are effectively assessed and optimized (multidimensional SAR) with the proteome-wide selectivity screening.

## Conclusion

A series of 5-substituted 7-phenyl-1-(oxazol-2-yl)heptan-1-ones was prepared and evaluated for FAAH inhibitory potency as well as FAAH selectivity versus competitive serine proteases (e.g., TGH, KIA1363). Aromatic and nonaromatic substituents were explored on the 5-position of the oxazole of **2f**, and many of these inhibitors approached or substantially exceeded its potency. Just as importantly, proteome-wide selectivity screening of the candidate inhibitors showed extraordinary selectivity for FAAH over all other serine hydrolases and proteases. Thus, addition of a C5 substituent to **20a** (R = H), which is 100-fold selective for TGH, results in inhibitors now selective for FAAH versus TGH. Most notable of these is the addition of a carboxylic acid either directly on the oxazole (**20b**) or on the 5-aryl group (e.g., **15r**) which imparts a 100−1000-fold selectivity for FAAH. For small, nonaryl substituents, a fundamental relationship between the $K_i$ and the electronic character of the substituent ($\sigma_p$) was defined that not only permits a prediction of the expected $K_i$, but also led to the design of FAAH inhibitors with $K_i$s as low as 400 pM. Finally, several of these inhibitors (**15q−t**, **20b**) contain substituents that would be expected to productively alter the physicochemical properties of **2f** and will facilitate their in vivo exploration.

## Experimental Section

**6-(2-(7-Phenylheptanoyl)oxazol-5-yl)picolinic Acid (15r).** 2-(1-(*tert*-Butyldimethylsilyloxy)-7-phenylheptyl)-5-(tributylstannyl)oxazole[47] (**5**, 1.27 g, 1.92 mmol), Pd(PPh₃)₄ (221 mg, 0.191 mmol), and methyl 6-chloropicolinate (658 mg, 3.83 mmol) were dissolved in anhydrous 1,4-dioxane (40 mL), and the mixture was warmed at reflux for 24 h under Ar. The mixture was diluted with EtOAc, washed with saturated aqueous NaCl, and dried over Na₂SO₄. Evaporation in vacuo yielded the crude product. Flash chromatography (SiO₂, 5−10% EtOAc/hexanes) yielded methyl 6-(2-(1-(*tert*-butyldimethylsilyloxy)-7-phenylheptyl)oxazol-5-yl)picolinate as a clear oil (975 mg, 100%): ¹H NMR (CDCl₃, 500 MHz) δ 8.12−8.10 (m, 1H), 7.99 (t, 1H, $J$ = 7.8 Hz), 7.90−7.89 (m, 1H), 7.86 (s, 1H), 7.35−7.32 (m, 2H), 7.25−7.22 (m, 3H), 4.94 (t, 1H, $J$ = 7.0 Hz), 4.10 (s, 3H), 2.67 (t, 2H, $J$ = 7.5 Hz), 2.04−1.96 (m, 2H), 1.74−1.67 (m, 2H), 1.55−1.39 (m, 6H), 0.97 (s, 9H), 0.17 (s, 3H), 0.07 (s, 1H); ¹³C NMR (CDCl₃, 125 MHz) δ 166.5, 165.8, 150.3, 148.7, 148.2, 143.3, 138.4, 128.8, 128.6, 126.8, 126.0, 124.3, 122.5, 69.2, 53.4, 36.8, 36.3, 31.8, 29.6, 26.1, 26.1, 25.5, 14.0, −4.5, −4.7.

Methyl 6-(2-(1-(*tert*-butyldimethylsilyloxy)-7-phenylheptyl)oxazol-5-yl)picolinate (1.95 g, 1.51 mmol) was dissolved in THF (30 mL), treated with Bu₄NF (1 M in THF, 4.6 mL, 1.81 mmol), and stirred at room temperature for 2 h under Ar. The reaction mixture was diluted with EtOAc, washed with saturated aqueous NaCl, and dried over Na₂SO₄. Evaporation in vacuo yielded the crude alcohol, which was filtered through a short silica gel pad. The silica gel pad was washed with 10% EtOAc/hexanes followed by 60% EtOAc/hexanes to afford the alcohol (1.24 g, 82%), which required no further purification. The alcohol (1.24 g, 3.14 mmol) was dissolved in CH₂Cl₂ (25 mL), and Dess−Martin periodinane (2.0 g, 4.72 mmol) was added. The mixture was stirred at room temperature for 2 h before silica gel was added, and the reaction mixture was evaporated in vacuo to afford the crude ketone absorbed on silica gel. Flash chromatography (SiO₂, 10−30% EtOAc) yielded methyl 6-(2-(7-phenylheptanoyl)oxazol-5-yl)pi-

colinate (**15n**) as a white solid (1.13 g, 91%): mp 50−51 °C; $^1$H NMR (CDCl$_3$, 500 MHz) $\delta$ 8.19 (d, 1H, $J$ = 7.0 Hz), 8.12−8.09 (m, 2H), 8.06−8.03 (m, 1H), 7.36−7.33 (m, 2H), 7.26−7.24 (m, 3H), 4.11 (s, 3H), 3.19 (t, 2H, $J$ = 7.0 Hz), 2.69 (t, 2H, $J$ = 7.5 Hz), 1.89−1.83 (m, 2H), 1.75−1.69 (m, 2H), 1.55−1.47 (m, 4H); $^{13}$C NMR (CDCl$_3$, 125 MHz) $\delta$ 188.9, 165.5, 158.0, 152.7, 149.0, 147.0, 143.1, 138.7, 128.8, 128.7, 128.4, 126.0, 125.6, 123.7, 53.5, 39.6, 36.3, 31.7, 29.4, 29.4, 24.3; ESI−TOF $m/z$ 393.1796 (M + H$^+$, C$_{23}$H$_{25}$N$_2$O$_4$, requires 393.1809).

Methyl 6-(2-(7-phenylheptanoyl)oxazol-5-yl)picolinate (**15n**, 1.13 g, 2.88 mmol) was dissolved in a mixture of 3:2 THF/H$_2$O (48 mL:32 mL), and LiOH (360 mg, 8.64 mmol) was added. The reaction mixture was stirred for 2 h at room temperature before the mixture was made acidic with the addition of aqueous 1 N HCl. The solution was diluted with EtOAc, and the organic layer was separated from the aqueous layer. The aqueous layer was extracted with EtOAc (3×). The combined organic extracts were washed with saturated aqueous NaCl and dried over Na$_2$SO$_4$. Evaporation in vacuo yielded the crude acid. Flash chromatography (SiO$_2$, 0−2% AcOH/EtOAc) yielded **15r** as a white solid (991 mg, 91%): mp 119−120 °C; $^1$H NMR (THF-$d_8$, 500 MHz) $\delta$ 8.11−8.04 (m, 4H), 7.22−7.08 (m, 5H), 3.08 (t, 2H, $J$ = 7.5 Hz), 2.61 (t, 2H, $J$ = 7.5 Hz), 1.76−1.68 (m, 2H), 1.68−1.62 (m, 2H), 1.45−1.41 (m, 4H); $^{13}$C NMR (THF-$d_8$, 125 MHz) $\delta$ 185.6, 163.1, 156.4, 151.4, 147.6, 144.7, 141.0, 137.1, 126.7, 126.5, 126.1, 123.9, 122.8, 121.1, 37.1, 34.3, 30.0, 27.6, 27.5, 22.2; ESI−TOF $m/z$ 379.1645 (M + H$^+$, C$_{22}$H$_{23}$N$_2$O$_4$, requires 379.1652).

**2-(7-Phenylheptanoyl)oxazole-5-carboxylic Acid (20b).** 2-(1-(*tert*-Butyldimethylsilyloxy)-7-phenylheptyl)oxazole[47] (**4**, 970 mg, 2.60 mmol) was dissolved in anhydrous THF (20 mL) and cooled to −78 °C, and *t*-BuLi (1.7 M in pentane, 1.99 mL, 3.38 mmol) was added dropwise under Ar. The reaction mixture was stirred for 2 h at −40 °C and recooled to −78 °C, and CO$_2$ (g) was bubbled through the solution for 1 h. The reaction mixture was warmed to room temperature, diluted with EtOAc, washed with saturated aqueous NaCl, and dried over Na$_2$SO$_4$. Evaporation in vacuo yielded the crude acid which was purified by flash chromatography (SiO$_2$, 0−2% AcOH/EtOAc gradient elution) to afford 2-(1-(*tert*-butyldimethylsilyloxy)-7-phenylheptyl)oxazole-5-carboxylic acid as a clear oil (921 mg, 85%): $^1$H NMR (CDCl$_3$, 500 MHz) $\delta$ 7.91 (s, 1H), 7.37−7.34 (m, 2H), 7.27−7.25 (m, 3H), 4.98 (t, 1H, $J$ = 7.0 Hz), 2.69 (t, 2H, $J$ = 7.5 Hz), 2.07−1.94 (m, 2H), 1.72−1.69 (m, 2H), 1.52−1.44 (m, 6H), 0.99 (s, 9H), 0.18 (s, 3H), 0.09 (s, 3H); $^{13}$C NMR (CDCl$_3$, 125 MHz) $\delta$ 169.3, 161.5, 143.1, 139.2, 134.5, 128.8, 128.7, 126.0, 126.3, 69.0, 36.8, 36.4, 31.8, 29.5, 26.1, 26.1, 25.4, 18.6, −4.6, −4.8.

2-(1-(*tert*-Butyldimethylsilyloxy)-7-phenylheptyl)oxazole-5-carboxylic acid (921 mg, 2.21 mmol) was dissolved in a mixture of MeOH:toluene (8 mL:20 mL) and cooled to 0 °C, and TMSCHN$_2$ (2 M in hexanes, 2.76 mL, 5.51 mmol) was added dropwise under Ar. The reaction mixture was stirred at room temperature for 0.5 h before it was cooled to 0 °C. Acetic acid was added dropwise until the solution turned from yellow to clear and bubbling ceased. The mixture was evaporated in vacuo, and the resulting solid was dissolved in EtOAc. The solution was washed with saturated aqueous NaHCO$_3$, washed with saturated aqueous NaCl, and dried over Na$_2$SO$_4$. Evaporation in vacuo yielded the crude product which was purified by flash chromatography (SiO$_2$, 10−30% EtOAc/ hexanes) to afford methyl 2-(1-(*tert*-butyldimethylsilyloxy)-7-phenylheptyl)oxazole-5-carboxylate as a white solid (831 mg, 90%): mp 38−39 °C; $^1$H NMR (CDCl$_3$, 500 MHz) $\delta$ 7.78 (s, 1H), 7.36−7.33 (m, 2H), 7.25−7.23 (m, 3H), 4.92 (t, 1H, $J$ = 7.0 Hz), 3.98 (s, 3H), 2.67 (t, 2H, $J$ = 7.5 Hz), 2.12−1.94 (m, 2H), 1.72−1.67 (m, 2H), 1.53−1.43 (m, 6H), 0.98 (s, 9H), 0.17 (s, 3H), 0.08 (s, 3H); $^{13}$C NMR (CDCl$_3$, 125 MHz) $\delta$ 169.0, 158.5, 143.1, 142.6, 134.5, 128.8, 128.6, 126.0, 69.1, 52.5, 36.7, 36.3, 31.8, 29.5, 26.1, 26.1, 25.4, 18.6, −4.6, −4.8.

Methyl 2-(1-(*tert*-butyldimethylsilyloxy)-7-phenylheptyl)oxazole-5-carboxylate (831 mg, 2.62 mmol) was dissolved in THF (10 mL), treated with Bu$_4$NF (1 M in THF, 2.31 mL, 3.14 mmol), and stirred at room temperature for 2 h under Ar. The reaction mixture was diluted with EtOAc, washed with saturated aqueous NaCl, and dried over Na$_2$SO$_4$. Evaporation in vacuo yielded the crude alcohol, which was filtered through a short silica gel pad. The silica gel pad was washed with 10% EtOAc/hexanes followed by 60% EtOAc/hexanes to afford the alcohol (559 mg, 91%) which required no further purification. The alcohol (544 mg, 1.71 mmol) was dissolved in CH$_2$Cl$_2$ (10 mL), and Dess−Martin periodinane (1.09 g, 2.57 mmol) was added. The mixture was stirred at room temperature for 2 h before silica gel was added, and the reaction mixture was evaporated in vacuo to afford the crude ketone absorbed on silica gel. Flash chromatography (SiO$_2$, 5−20% EtOAc/ hexanes) yielded methyl 2-(7-phenylheptanoyl)oxazole-5-carboxylate (**20c**) as a white solid (473 mg, 87%): mp 90−91 °C; $^1$H NMR (CDCl$_3$, 400 MHz) $\delta$ 7.84 (s, 1H), 7.25−7.21 (m, 2H), 7.15−7.12 (m, 3H), 3.93 (s, 3H), 3.04 (t, 2H, $J$ = 7.5 Hz), 2.57 (t, 2H, $J$ = 7.5 Hz), 1.76−1.68 (m, 2H), 1.63−1.56 (m, 2H), 1.42−1.32 (m, 4H); $^{13}$C NMR (CDCl$_3$, 100 MHz) $\delta$ 188.4, 158.5, 157.7, 143.9, 142.8, 134.8, 128.6, 128.4, 125.8, 53.0, 39.7, 36.0, 31.4, 29.1, 29.1, 23.7; ESI−TOF $m/z$ 316.1533 (M + H$^+$, C$_{18}$H$_{22}$NO$_4$, requires 316.1543).

Methyl 2-(7-phenylheptanoyl)oxazole-5-carboxylate (**20c**, 71 mg, 0.225 mmol) was dissolved in a mixture of 3:2 THF/H$_2$O (6 mL:4 mL), and LiOH (28 mg, 0.672 mmol) was added. The reaction mixture stirred for 2 h at room temperature before the mixture was made acidic with the addition of aqueous 1 N HCl. The solution was diluted with EtOAc, and the organic layer was separated from the aqueous layer. The aqueous layer was extracted with EtOAc. The combined organic extracts were washed with saturated aqueous NaCl and dried over Na$_2$SO$_4$. Evaporation in vacuo yielded the crude acid. Flash chromatography (SiO$_2$, 0−2% AcOH/EtOAc gradient elution) yielded **20b** as a white solid (60 mg, 88%): mp 47−48 °C; $^1$H NMR (CD$_3$OD, 600 MHz) $\delta$ 7.62 (s, 1H), 7.22−7.19 (m, 2H), 7.14−7.09 (m, 3H), 3.04 (t, 2H, $J$ = 7.5 Hz), 2.58 (t, 2H, $J$ = 7.5 Hz), 1.71−1.68 (m, 2H), 1.62−1.59 (m, 2H), 1.41−1.32 (m, 4H); $^{13}$C NMR (CD$_3$OD, 150 MHz) $\delta$ 189.0, 159.4, 159.4, 143.3, 143.3, 134.6, 128.9, 128.7, 126.1, 39.6, 36.3, 32.0, 29.5, 29.4, 23.9; ESI−TOF $m/z$ 302.1382 (M + H$^+$, C$_{17}$H$_{20}$NO$_4$, requires 302.1387).

**FAAH Inhibition.** $^{14}$C-Labeled oleamide was prepared from $^{14}$C-labeled oleic acid as described.[4,55] The truncated rat FAAH (rFAAH) was expressed in *E. coli* and purified as described.[76] The purified recombinant rFAAH was used in the inhibition assays unless otherwise indicated. The full-length human FAAH (hFAAH) was expressed in COS-7 cells as described,[32] and the lysate of hFAAH-transfected COS-7 cells was used in the inhibition assays where explicitly indicated.

The inhibition assays were performed as described.[4,55] In brief, the enzyme reaction was initiated by mixing 1 nM of rFAAH (800, 500, or 200 pM rFAAH for inhibitors with $K_i \leq 1−2$ nM) with 10 $\mu$M of $^{14}$C-labeled oleamide in 500 $\mu$L of reaction buffer (125 mM TrisCl, 1 mM EDTA, 0.2% glycerol, 0.02% Triton X-100, 0.4 mM HEPES, pH 9.0) at room temperature in the presence of three different concentrations of inhibitor. The enzyme reaction was terminated by transferring 20 $\mu$L of the reaction mixture to 500 $\mu$L of 0.1 N HCl at three different time points. The $^{14}$C-labeled oleamide (substrate) and oleic acid (product) were extracted with EtOAc and analyzed by TLC as detailed.[4,55] The $K_i$ of the inhibitor was calculated using a Dixon plot as described (standard deviations are provided in the Supporting Information tables).[47] Lineweaver−Burk analysis was performed as described,[4,55] in the presence or absence of 8 nM of **2f**, respectively, confirming competitive, reversible inhibition.[45]

**Selectivity Screening.** The selectivity screening was conducted as detailed.[69]

**Supporting Information Available:** Full experimental details and characterization, FAAH assay measurement errors, and purities (HPLC analysis) of the FAAH inhibitors disclosed herein. This material is available free of charge via the Internet at http://pubs.acs.org.

## References

(1) Devane, W. A.; Hanus, L.; Breuer, A.; Pertwee, R. G.; Stevenson, L. A.; Griffin, G.; Gibson, D.; Mandelbaum, A.; Etinger, A.; Mechoulam, R. Isolation and Structure of a Brain Constituent that Binds to the Cannabinoid Receptor. *Science* **1992**, *258*, 1946−1949.

(2) Boger, D. L.; Henriksen, S. J.; Cravatt, B. F. Oleamide: An Endogenous Sleep-Inducing Lipid and Prototypical Member of a New Class of Lipid Signalling Molecules. *Curr. Pharm. Des.* **1998**, *4*, 303−314.

(3) Cravatt, B. F.; Lerner, R. A.; Boger, D. L. Structure Determination of an Endogenous Sleep-Inducing Lipid, cis-9-Octadecenamide (Oleamide): A Synthetic Approach to the Chemical Analysis of Trace Quantitites of a Natural Product. *J. Am. Chem. Soc.* **1996**, *118*, 580−590.

(4) Cravatt, B. F.; Prospero-Garcia, O.; Suizdak, G.; Gilula, N. B.; Henriksen, S. J.; Boger, D. L.; Lerner, R. A. Chemical Characterization of a Family of Brain Lipids that Induce Sleep. *Science* **1995**, *268*, 1506−1509.

(5) Schmid, H. H. O.; Schmid, P. C.; Natarajan, V. *N*-Acylated Glycerophospholipids and Their Derivatives. *Prog. Lipid Res.* **1990**, *29*, 1−43.

(6) Lambert, D. M.; Fowler, C. J. The Endocannabinoid System: Drug Targets, Lead Compounds, and Potential Therapeutic Applications. *J. Med. Chem.* **2005**, *48*, 5059−5087.

(7) Calignano, A.; La Rana, G.; Giuffrida, A.; Piomelli, D. Control of Pain Initiation by Endogenous Cannabinoids. *Nature* **1998**, *394*, 277−281.

(8) Cravatt, B. F.; Lichtman, A. H. The Endogenous Cannabinoid System and Its Role in Nociceptive Behavior. *J. Neurobiol.* **2004**, *61*, 149−160.

(9) Walker, J. M.; Huang, S. M.; Stragman, N. M.; Tsou, K.; Sanudo-Pena, M. C. Pain Modulation by Release of the Endogenous Cannabinoid Anandamide. *Proc. Natl. Acad. Sci. U.S.A.* **1999**, *96*, 12198−12203.

(10) Gomez, R.; Navarro, M.; Ferrer, B.; Trigo, J. M.; Bilbao, A.; Del Arco, I.; Cippitelli, A.; Nava, F.; Piomelli, D.; Rodríguez de Fonseca, F. A Peripheral Mechanism for CB1 Cannabinoid Receptor Dependent Modulation of Feeding. *J. Neurosci.* **2002**, *22*, 9612−9617.

(11) Williams, C. M.; Kirkham, T. C. Observational Analysis of Feeding Induced by Δ-THC and Anandamide. *Physiol. Behav.* **2002**, *76*, 241−250.

(12) Kathuria, S.; Gaetani, S.; Fegley, D.; Valino, F.; Duranti, A.; Tontini, A.; Mor, M.; Tarzia, G.; La Rana, G.; Calignano, A.; Giustino, A.; Tattoli, M.; Palmery, M.; Cuomo, V.; Piomelli, D. Modulation of Anxiety Through Blockade of Anandamide Hydrolysis. *Nat. Med.* **2003**, *9*, 76−81.

(13) Melck, D.; Rueda, D.; Galve-Roberh, I.; De Petrocellis, L.; Guzmán, M.; Di Marzo, V. Involvement of the cAMP/Protein Kinase A Pathway and of Mitogen-Activated Protein Kinase in the Anti-Proliferative Effects of Anandamide in Human Breast Cancer Cells. *FEBS Lett.* **1999**, *463*, 235−240.

(14) Yamaji, K.; Sarker, K. P.; Kawahara, K.; Iino, S.; Yamakuchi, M.; Abeyama, K.; Hashiguchi, T.; Maruyama, I. Anandamide Induces Apoptosis in Human Endothelial Cells: Its Regulation System and Clinical Implications. *Thromb. Haemostasis* **2003**, *89*, 875−884.

(15) Massa, F.; Marsicano, G.; Hermann, H.; Cannich, A.; Monory, K.; Cravatt, B. F.; Ferri, G. L.; Sibaev, A.; Storr, M.; Lutz, B. The Endogenous Cannabinoid System Protects Against Colonic Inflammation. *J. Clin. Invest.* **2004**, *113*, 1202−1209.

(16) Mallet, P. E.; Beninger, R. J. The Cannabinoid CB1 Receptor Antagonist SR141716A Attenuates the Memory Impairment Produced by Δ9-Tetrahydrocannabinol or Anandamide. *Psychopharmacology* **1998**, *140*, 11−19.

(17) Panikashvili, D.; Simeonidou, C.; Ben Shabat, S.; Hanus, L.; Breuer, A.; Mechoulam, R.; Shohami, E. An Endogenous Cannabinoid (2-AG) is Neuroprotective after Brain Injury. *Nature* **2001**, *413*, 527−531.

(18) Axelrod, J.; Felder, C. C. Cannabinoid Receptors and Their Endogenous Agonist, Anandamide. *Neurochem. Res.* **1998**, *23*, 575−581.

(19) Di Marzo, V.; Bisogno, T.; De Petrocellis, L.; Melck, D.; Martin, B. R. Cannabimimetic Fatty Acid Derivatives: The Anandamide Family and Other "Endocannabinoids". *Curr. Med. Chem.* **1999**, *6*, 721−744.

(20) Martin, B. R.; Mechoulam, R.; Razdan, R. K. Discovery and Characterization of Endogenous Cannabinoids. *Life Sci.* **1999**, *65*, 573−595.

(21) Cheer, J. F.; Cadogan, A.-K.; Marsden, C. A.; Fone, K. C. F.; Kendall, D. A. Modification of 5-HT2 Receptor Mediated Behaviour in the Rat by Oleamide and the Role of Cannabinoid Receptors. *Neuropharmacology* **1999**, *38*, 533−541.

(22) Thomas, E. A.; Cravatt, B. F.; Sutcliffe, J. G. The Endogenous Lipid Oleamide Activates Serotonin 5-HT7 Neurons in Mouse Thalamus and Hypothalamus. *J. Neurochem.* **1999**, *72*, 2370−2378.

(23) Boger, D. L.; Patterson, J. E.; Jin, Q. Structural Requirements for 5-HT2A and 5-HT1A Receptor Potentiation by the Biologically Active Lipid Oleamide. *Proc. Natl. Acad. Sci. U.S.A.* **1998**, *95*, 4102−4107.

(24) Lees, G.; Dougalis, A. Differential Effects of the Sleep-Inducing Lipid Oleamide and Cannabinoids on the Induction of Long-Term Potentiation in the CA1 Neurons of the Rat Hippocampus In Vitro. *Brain Res.* **2004**, *997*, 1−14.

(25) Yost, C. S.; Hampson, A. J.; Leonoudakis, D.; Koblin, D. D.; Bornheim, L. M.; Gray, A. T. Oleamide Potentiates Benzodiazepine-Sensitive γ-Aminobutyric Acid Receptor Activity But Does Not Alter Minimum Alveolar Anesthetic Concentration. *Anesth. Analg.* **1998**, *86*, 1294−1299.

(26) Boger, D. L.; Patterson, J. E.; Guan, X.; Cravatt, B. F.; Lerner, R. A.; Gilula, N. B. Chemical Requirements for Inhibition of Gap Junction Communication by the Biologically Active Lipid Oleamide. *Proc. Natl. Acad. Sci. U.S.A.* **1998**, *95*, 4810−4815.

(27) Guan, X.; Cravatt, B. F.; Ehring, G. R.; Hall, J. E.; Boger, D. L.; Lerner, R. A.; Gilula, N. B. The Sleep-Inducing Lipid Oleamide Deconvolutes Gap Junction Communication and Calcium Wave Transmission in Glial Cells. *J. Cell Biol.* **1997**, *139*, 1785−1792.

(28) Huitrón-Reséndiz, S.; Gombart, L.; Cravatt, B. F.; Henriksen, S. J. Effect of Oleamide on Sleep and its Relationship to Blood Pressure, Body Temperature, and Locomotor Activity in Rats. *Exp. Neurol.* **2001**, *172*, 235−243.

(29) Mechoulam, R.; Fride, E.; Hanus, L.; Sheskin, T.; Bisogno, T.; Di Marzo, V.; Bayewitch, M.; Vogel, Z. Anandamide May Mediate Sleep Induction. *Nature* **1997**, *389*, 25−26.

(30) Bracey, M. H.; Hanson, M. A.; Masuda, K. R.; Stevens, R. C.; Cravatt, B. F. Structural Adaptations in a Membrane Enzyme that Terminates Endocannabinoid Signaling. *Science* **2002**, *298*, 1793−1796.

(31) Cravatt, B. F.; Giang, D. K.; Mayfield, S. P.; Boger, D. L.; Lerner, R. A.; Gilula, N. B. Molecular Characterization of an Enzyme that Degrades Neuromodulatory Fatty-Acid Amides. *Nature* **1996**, *384*, 83−87.

(32) Giang, D. K.; Cravatt, B. F. Molecular Characterization of Human and Mouse Fatty Acid Amide Hydrolases. *Proc. Natl. Acad. Sci. U.S.A.* **1997**, *94*, 2238−2242.

(33) Patricelli, M. P.; Cravatt, B. F. Proteins Regulating the Biosynthesis and Inactivation of Neuromodulatory Fatty Acid Amides. *Vit. Hormones* **2001**, *62*, 95−131.

(34) Boger, D. L.; Fecik, R. A.; Patterson, J. E.; Miyauchi, H.; Patricelli, M. P.; Cravatt, B. F. Fatty Acid Amide Hydrolase Substrate Specificity. *Bioorg. Med. Chem. Lett.* **2000**, *10*, 2613−2616.

(35) Lang, W.; Qin, C.; Lin, S.; Khanolkar, A. D.; Goutopoulos, A.; Fan, P.; Abouzid, K.; Meng, Z.; Biegel, D.; Makriyannis, A. Substrate Specificity and Stereoselectivity of Rat Brain Microsomal Anandamide Amidohydrolase. *J. Med. Chem.* **1999**, *42*, 896−902.

(36) Egertova, M.; Cravatt, B. F.; Elphick, M. R. Comparative Analysis of Fatty Acid Amide Hydrolase and CB1 Cannabinoid Receptor Expression in the Mouse Brain: Evidence of a Widespread Role for Fatty Acid Amide Hydrolase in Regulation of Endocannabinoid Signaling. *Neuroscience* **2003**, *119*, 481−496.

(37) Patricelli, M. P.; Cravatt, B. F. Fatty Acid Amide Hydrolase Competitively Degrades Bioactive Amides and Esters Through a Nonconventional Catalytic Mechanism. *Biochemistry* **1999**, *38*, 14125−14130.

(38) Patricelli, M. P.; Cravatt, B. F. Clarifying the Catalytic Roles of Conserved Residues in the Amidase Signature Family. *J. Biol. Chem.* **2000**, *275*, 19177−19184.

(39) Patricelli, M. P.; Lovato, M. A.; Cravatt, B. F. Chemical and Mutagenic Investigations of Fatty Acid Amide Hydrolase: Evidence for a Family of Serine Hydrolases with Distinct Catalytic Properties. *Biochemistry* **1999**, *38*, 9804−9812.

(40) Clement, A. B.; Hawkins, E. G.; Lichtman, A. H.; Cravatt, B. F. Increased Seizure Susceptibility and Proconvulsant Activity of Anandamide in Mice Lacking Fatty Acid Amide Hydrolase. *J. Neurosci.* **2003**, *23*, 3916−3923.

(41) Cravatt, B. F.; Demarest, K.; Patricelli, M. P.; Bracey, M. H.; Giang, D. K.; Martin, B. R.; Lichtman, A. H. Supersensitivity to Anandamide and Enhanced Endogenous Cannabinoid Signaling in Mice Lacking Fatty Acid Amide Hydrolase. *Proc. Natl. Acad. Sci. U.S.A.* **2001**, *98*, 9371–9376.

(42) Cravatt, B. F.; Saghatelian, A.; Hawkins, E. G.; Clement, A. B.; Bracey, M. H.; Lichtman, A. H. Functional Disassociation of the Central and Peripheral Fatty Acid Amide Signaling Systems. *Proc. Natl. Acad. Sci. U.S.A.* **2004**, *101*, 10821–10826.

(43) Lichtman, A. H.; Shelton, C. C.; Advani, T.; Cravatt, B. F. Mice Lacking Fatty Acid Amide Hydrolase Exhibit a Cannabinoid Receptor-Mediated Phenotypic Hypoalgesia. *Pain* **2004**, *109*, 319–327.

(44) Cravatt, B. F.; Lichtman, A. H. Fatty Acid Amide Hydrolase: An Emerging Therapeutic Target in the Endocannabinoid System. *Curr. Opin. Chem. Biol.* **2003**, *7*, 469–475.

(45) Boger, D. L.; Miyauchi, H.; Du, W.; Hardouin, C.; Fecik, R. A.; Cheng, H.; Hwang, I.; Hedrick, M. P.; Leung, D.; Acevedo, O.; Guimaráes, C. R. W.; Jorgensen, W. L.; Cravatt, B. F. Discovery of a Potent, Selective, and Efficacious Class of Reversible α-Ketoheterocycle Inhibitors of Fatty Acid Amide Hydrolase as Analgesics. *J. Med. Chem.* **2005**, *48*, 1849–1856.

(46) Boger, D. L.; Sato, H.; Lerner, A. E.; Austin, B. J.; Patterson, J. E.; Patricelli, M. P.; Cravatt, B. F. Trifluoromethyl Ketone Inhibitors of Fatty Acid Amide Hydrolase: A Probe of Structural and Conformational Features Contributing to Inhibition. *Bioorg. Med. Chem. Lett.* **1999**, *9*, 265–270.

(47) Boger, D. L.; Sato, H.; Lerner, A. E.; Hedrick, M. P.; Fecik, R. A.; Miyauchi, H.; Wilkie, G. D.; Austin, B. J.; Patricelli, M. P.; Cravatt, B. F. Exceptionally Potent Inhibitors of Fatty Acid Amide Hydrolase: The Enzyme Responsible for Degradation of Endogenous Oleamide and Anandamide. *Proc. Natl. Acad. Sci. U.S.A.* **2000**, *97*, 5044–5049.

(48) De Petrocellis, L.; Melck, D.; Ueda, N.; Maurelli, S.; Kurahashi, Y.; Yamamoto, S.; Marino, G.; Di Marzo, V. Novel Inhibitors of Brain, Neuronal, and Basophilic Anandamide Amidohydrolase. *Biochem. Biophys. Res. Commun.* **1997**, *231*, 82–88.

(49) Deutsch, D. G.; Omeir, R.; Arreaza, G.; Salehani, D.; Prestwich, G. D.; Huang, Z.; Howlett, A. Methyl Arachidonyl Fluorophosphonate: A Potent Irreversible Inhibitor of Anandamide Amidase. *Biochem. Pharmacol.* **1997**, *53*, 255–260.

(50) Deutsch, D. G.; Lin, S.; Hill, W. A. G.; Morse, K. L.; Salehani, D.; Arreaza, G.; Omeir, R. L.; Makriyannis, A. Fatty Acid Sulfonyl Fluorides Inhibit Anandamide Metabolism and Bind to the Cannabinoid Receptor. *Biochem. Biophys. Res. Commun.* **1997**, *231*, 217–221.

(51) Du, W.; Hardouin, C.; Cheng, H.; Hwang, I.; Boger, D. L. Heterocyclic Sulfoxide and Sulfone Inhibitors of Fatty Acid Amide Hydrolase. *Bioorg. Med. Chem. Lett.* **2005**, *15*, 103–106.

(52) Edgemond, W. S.; Greenberg, M. J.; McGinley, P. J.; Muthians, S.; Campbell, W. B.; Hillard, C. J. Synthesis and Characterization of Diazomethylarachidonyl Ketone: An Irreversible Inhibitor of N-Arachidonylethanolamine Amidohydrolase. *J. Pharmacol. Exp. Ther.* **1998**, *286*, 184–190.

(53) Fernando, S. R.; Pertwee, R. G. Evidence that Methyl Arachidonyl Fluorophosphonate is an Irreversible Cannabinoid Receptor Antagonist. *Br. J. Pharmacol.* **1997**, *121*, 1716–1720.

(54) Koutek, B.; Prestwich, G. D.; Howlett, A. C.; Chin, S. A.; Salehani, D.; Akhavan, N.; Deutsch, D. G. Inhibitors of Arachidonoyl Ethanolamide Hydrolysis. *J. Biol. Chem.* **1994**, *269*.

(55) Patricelli, M. P.; Patterson, J. P.; Boger, D. L.; Cravatt, B. F. An Endogenous Sleep-Inducing Compound is a Novel Competitive Inhibitor of Fatty Acid Amide Hydrolase. *Bioorg. Med. Chem. Lett.* **1998**, *8*, 613–618.

(56) Patterson, J. E.; Ollmann, I. R.; Cravatt, B. F.; Boger, D. L.; Wong, C.-H.; Lerner, R. A. Inhibition of Oleamide Hydrolase Catalyzed Hydrolysis of the Endogenous Sleep-Inducing Lipid *cis*-9-Octadecenamide. *J. Am. Chem. Soc.* **1996**, *118*, 5938–5945.

(57) Tarzia, G.; Duranti, A.; Gatti, G.; Piersanti, G.; Tontini, A.; Rivara, S.; Lodola, A.; Plazzi, P. V.; Mor, M.; Kathuria, S.; Piomelli, D. Synthesis and Structure–Activity Relationships of FAAH Inhibitors: Cyclohexylcarbamic Acid Biphenyl Esters with Chemical Modulation at the Proximal Phenyl Ring. *ChemMedChem* **2006**, *1*, 130–139.

(58) Tarzia, G.; Duranti, A.; Tontini, A.; Piersanti, G.; Mor, M.; Rivara, S.; Plazzi, P. V.; Park, C.; Kathuria, S.; Piomelli, D. Design, Synthesis, and Structure-Activity Relationships of Alkylcarbamic Acid Aryl Esters, a New Class of Fatty Acid Amide Hydrolase Inhibitors. *J. Med. Chem.* **2003**, *46*, 2352–2360.

(59) Mor, M.; Rivara, S.; Lodola, A.; Plazzi, P. V.; Tarzia, G.; Duranti, A.; Tontini, A.; Piersanti, G.; Kathuria, S.; Piomelli, D. Cyclohexylcarbamic Acid 3′- or 4′-Substituted Biphenyl-3-yl Esters as Fatty Acid Amide Hydrolase Inhibitors: Synthesis, Quantitative Structure–Activity Relationships, and Molecular Modeling Studies. *J. Med. Chem.* **2004**, *47*, 4998–5008.

(60) Muccioli, G. G.; Fazio, N.; Scriba, G. K. E.; Poppitz, W.; Cannata, F.; Poupaert, J. H.; Wouters, J.; Lambert, D. M. Substituted 2-Thioxoimidazolidin-4-ones and Imidazolidine-2,4-diones as Fatty Acid Amide Hydrolase Inhibitors Templates. *J. Med. Chem.* **2006**, *49*, 417–425.

(61) Romero, F. A.; Hwang, I.; Boger, D. L. Delineation of a Fundamental α-Ketoheterocycle Substituent Effect For Use in the Design of Enzyme Inhibitors. *J. Am. Chem. Soc.* **2006**, *128*, 14004–14005.

(62) Leung, D.; Du, W.; Hardouin, C.; Cheng, H.; Hwang, I.; Cravatt, B. F.; Boger, D. L. Discovery of an Exceptionally Potent and Selective Class of Fatty Acid Amide Hydrolase Inhibitors Enlisting Proteome-Wide Selectivity Screening: Concurrent Optimization of Enzyme Inhibitor Potency and Selectivity. *Bioorg. Med. Chem. Lett.* **2005**, *15*, 1423–1428.

(63) Hohmann, A. G.; Suplita, R. L.; Bolton, N. M.; Neeley, M. H.; Fegley, D.; Mangieri, R.; Krey, J.; Walker, J. M.; Holmes, P. V.; Crystal, J. D.; Duranti, A.; Tontini, A.; Mor, M.; Tarzia, G.; Piomelli, D. An Endocannabinoid Mechanism for Stress-Induced Analgesia. *Nature* **2005**, *435*, 1108–1112.

(64) Alexander, J. P.; Cravatt, B. F. The Putative Endocannabinoid Transport Blocker LY2183240 Is a Potent Inhibitor of FAAH and Several Other Brain Serine Hydrolases. *J. Am. Chem. Soc.* **2006**, *128*, 9699–9704.

(65) Alexander, J. P.; Cravatt, B. F. Mechanism of Carbamate Inactivation of FAAH: Implications for the Design of Covalent Inhibitors and In Vivo Functional Probes for Enzymes. *Chem. Biol.* **2005**, *12*, 1179–1187.

(66) Lichtman, A. H.; Leung, D.; Shelton, C. C.; Saghatelian, A.; Hardouin, C.; Boger, D. L.; Cravatt, B. F. Reversible Inhibitors of Fatty Acid Amide Hydrolase that Promote Analgesia: Evidence for an Unprecedented Combination of Potency and Selectivity. *J. Pharmacol. Exp. Ther.* **2004**, *311*, 441–448.

(67) Boger, D. L.; Miyauchi, H.; Hedrick, M. P. α-Keto Heterocycle Inhibitors of Fatty Acid Amide Hydrolase: Carbonyl Group Modification and α-Substitution. *Bioorg. Med. Chem. Lett.* **2001**, *11*, 1517–1520.

(68) Chang, L.; Luo, L.; Palmer, J. A.; Sutton, S.; Wilson, S. J.; Barbier, A. J.; Breitenbucher, J. G.; Chaplan, S. R.; Webb, M. Inhibition of Fatty Acid Amide Hydrolase Produces Analgesia by Multiple Mechanisms. *Br. J. Pharmacol.* **2006**, *148*, 102–113.

(69) Leung, D.; Hardouin, C.; Boger, D. L.; Cravatt, B. F. Discovering Potent and Selective Reversible Inhibitors of Enzymes in Complex Proteomes. *Nature Biotechnol.* **2003**, *21*, 687–691.

(70) Vedejs, E.; Monahan, S. D. Metalation of Oxazole–Borane Complexes: A Practical Solution to the Problem of Electrocyclic Ring Opening of 2-Lithiooxazoles. *J. Org. Chem.* **1996**, *61*, 5192–5193.

(71) Hari, Y.; Obika, S.; Sakaki, M.; Morio, K.; Yamagata, Y.; Imanishi, T. Effective Synthesis of C-Nucleosides with 2′,4′-BNA Modification. *Tetrahedron* **2002**, *58*, 3051–3063.

(72) Farina, V.; Krishnamurthy, V.; Scott, W. J. The Stille Reaction. *Org. React.* **1997**, *50*, 1–652.

(73) Dess, D. B.; Martin, J. C. A Useful 12-I-5 Triacetoxyperiodinane (the Dess-Martin periodinane) for the Selective Oxidation of Primary or Secondary Alcohols and a Variety of Related 12-I-5 Species. *J. Am. Chem. Soc.* **1991**, *113*, 7277–7287.

(74) Chen, Q.-Y.; Wu, S.-W. Methyl Fluorosulphonyldifluoroacetate; A New Trifluoromethylating Agent. *J. Chem. Soc., Chem. Commun.* **1989**, 705–706.

(75) Qing, F.-L.; Fan, J.; Sun, H.-B.; Yue, X.-J. First Synthesis of *ortho*-Trifluoromethylated Aryl Triflates. *J. Chem. Soc., Perkin Trans. 1* **1997**, 3053–3057.

(76) Patricelli, M. P.; Lashuel, H. A.; Giang, D. K.; Kelly, J. W.; Cravatt, B. F. Comparative Characterization of a Wild Type and Transmembrane Domain-Deleted Fatty Acid Amide Hydrolase: Identification of the Transmembrane Domain as a Site for Oligomerization. *Biochemistry* **1998**, *37*, 15177–15187.

(77) Guimaráes, C. R. W.; Boger, D. L.; Jorgensen, W. L. Elucidation of Fatty Acid Amide Hydrolase Inhibition by Potent α-Ketoheterocycle Derivatives from Monte Carlo Simulations. *J. Am. Chem. Soc.* **2005**, *127*, 17377–17384.

(78) Edwards, P. D.; Zottola, M. A.; Davis, M.; Williams, C. M.; Tuthill, P. A. Peptidyl α-Ketoheterocyclic Inhibitors of Human Neutrophil Elastase. 3. In Vitro Potency and in Vivo Potency of a Series of Peptidyl α-Ketobenzoxazoles. *J. Med. Chem.* **1995**, *38*, 3972–3982.

(79) Edwards, P. D.; Zottola, M. A.; Davis, M.; Williams, J.; Tuthill, P. A. Peptidyl α-Ketoheterocyclic Inhibitors of Human Neutrophil Elastase. 2. Effect of Varying the Heterocyclic Ring on in Vitro Potency. *J. Med. Chem.* **1995**, *38*, 76−85.

(80) Costanzo, M. J.; Almond, H. R.; Hecker, L. R.; Schott, M. R.; Yabut, S. C.; Zhang, H.-C.; Andrade-Gordon, P.; Corcoran, T. W.; Giardino, E. C.; Kauffman, J. A.; Lewis, J. M.; de Garavilla, L.; Haertlein, B. J.; Maryanoff, B. E. In-Depth Study of Tripeptide-Based α-Ketoheterocycles as Inhibitors of Thrombin. Effective Utilization of the S1′ Subsite and Its Implications to Structure-Based Drug Design. *J. Med. Chem.* **2005**, *48*, 1984−2008.